MESON SPECTROSCOPY*

F. Wagner

Lawrence Berkeley Laboratory
University of California
Berkeley, California 94720

and

Max-Planck Institut für Physik, Munich

July 1974

I. INTRODUCTION

The progress made in the last few years in meson spectroscopy is illustrated in Fig. 1, which shows the number of mesons listed in the PDG tables versus year (dashed line). The states with known quantum numbers are indicated by a solid line. The former is about constant, showing the increasingly conservative attitude of PDG in time, whereas the latter has almost doubled during the last three years. This progress is mainly due to the appearance of high statistics experiments allowing in many cases a detailed phase shift analysis. At the same time the production mechanism of those mesons has been understood. The importance of this connection between what and how something is produced has been emphasized by Fox et al.[1] and recently by Kane.[2] I will illustrate the progress made in the case of $\pi\pi$ and $K\pi$ elastic scattering (Section II) and the 3π and $K\pi\pi$ analyses (Section III). Section IV discusses formation experiments in $N\bar{N}$, and Section V contains miscellaneous results.

II. $\pi\pi$ AND $K\pi$ ELASTIC SCATTERING

Apart from minor sources (like K_{e4}) the main information of $\pi\pi$ and $K\pi$ scattering comes from the so-called Chew-Low Extrapolation.[3] Measuring the cross section for $\pi A \to \pi\pi A'$, one can obtain by performing the limit

$$d\sigma(\pi\pi \to \pi\pi) = \lim_{t \to m_\pi^2} \left| \frac{t-m_\pi^2}{V_{\pi AA'}} \right|^2 d\sigma(\pi A \to \pi\pi A') \qquad (2.1)$$

the $\pi\pi$ cross section (t is the momentum transfer between A and A', and

*Work supported in part by the U. S. Atomic Energy Commission.

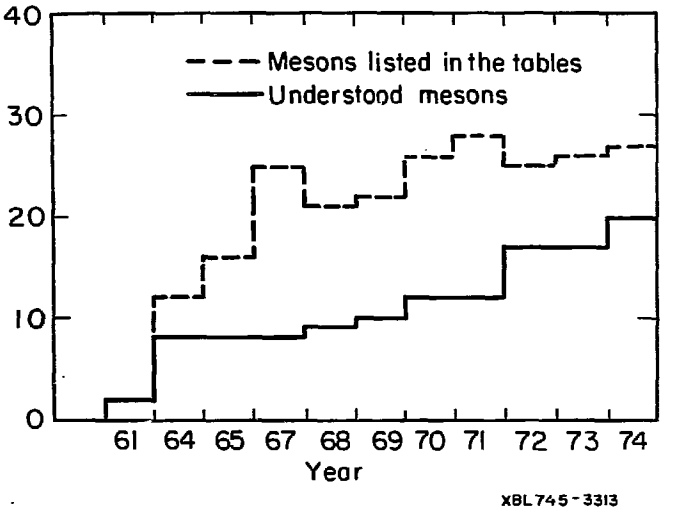

FIG. 1. Number of meson states listed in the PDG tables each year (dashed line). The number of states with known quantum numbers is indicated by a solid line.

$V(t)_{\pi AA'}$ the $\pi AA'$ vertex]. In the physical region other exchanges contribute, as the appearance of $M \neq 0$ $\pi\pi$ decay moments in the t-channel helicity system (THS) shows, and therefore a precise extrapolation requires the understanding also of the non-π-exchange amplitudes.

A. $\pi\pi$ below 1 GeV

The old question of the so-called up-down ambiguity of the $I = 0$ $\pi\pi$ S-wave above the ρ-meson was resolved two years ago by Protopopescu et al.[4] in favor of the down solution by extrapolating the reactions

$$\pi^+ p \rightarrow \pi^+ \pi^- \Delta^{++}, \tag{2.2}$$

$$\pi^+ p \rightarrow K^+ K^- \Delta^{++} \tag{2.3}$$

according to Eq. (2.1). As we will see later, this can be justified in this case. Last year the result[5] of a high-statistics experiment of the CERN-MUNICH spectrometer for

$$\pi^- p \rightarrow \pi^- \pi^+ n \tag{2.4}$$

at 17 GeV/c (300K events) and this year[6] at 7 GeV/c (40K events) had become available. The measurement at the lower beam momentum has been done because of the much better acceptance at low $\pi\pi$ masses. The moments $\langle Y_M^L \rangle$ in the ρ region at 17 GeV/c as a function of $\sqrt{-t}$ are shown in Fig. 2. One sees that large $M = 1$ moments in the THS occur. More seriously, all moments are almost constant as a function of $\sqrt{-t}$ below $|t| \leq 0.15\,\mathrm{GeV}^2$, which makes a simple extrapolation according to (2.1) prohibitive. Therefore additional assumptions have to be made. All analyses done on the CERN-MUNICH data are more or less motivated by the following simple model, the so-called electric Born term model (EBTM).[7] It leads to the same amplitudes as the poor man's absorption model.[8] To the π-exchange graph (OPE) one adds the nucleon Born terms as

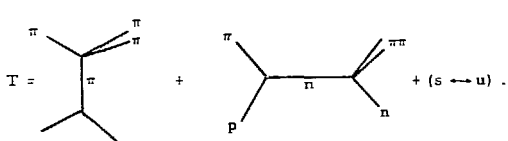

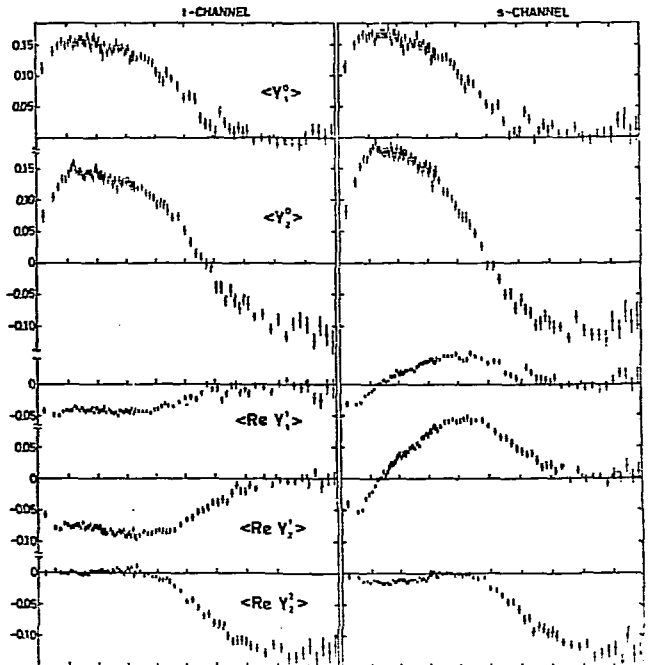

FIG. 2. The $\pi\pi$ moments as function of $\sqrt{-t}$ in the ρ region ($0.71 < M_{\pi\pi} < 0.83$ GeV) from the reaction $\pi^- p \to \pi^-\pi^+ n$ at 17 GeV/c[5] for the s- and t-channel helicity system.

At small $|t|$ A_2-exchange can be neglected. The graphs (2.5) lead to the following predictions for the ratio of $\pi\pi$ moments (SHS) at high energies:

$$\langle Y_1^2\rangle/\langle Y_2^2\rangle = \frac{m_{\pi\pi}}{2m_\pi^2}\ \frac{t+m_\pi^2}{\sqrt{-t}}\ ,$$

$$\langle Y_1^2\rangle/\langle Y_0^2\rangle = \sqrt{\frac{-3t}{2}}\ \frac{t+m_\pi^2}{t^2+m_{\pi\pi}^2\cdot t+m_\pi^4}\ . \qquad (2.6)$$

$$\langle Y_1^1\rangle/\langle Y_0^1\rangle = -\frac{t+m_\pi^2}{m_{\pi\pi}}\ \frac{1}{\sqrt{-2t}}\ .$$

As Fig. 3 shows, these predictions are in excellent agreement with the data.[5] The zero at $t = m_\pi^2$ is nicely reproduced. Other properties of this model are:

SC: only nucleon flip in the SHS occurs, therefore one has spin coherence at the nucleon vertex.

PC: Since the Born terms are real, amplitudes with the same angular momentum l of the $\pi\pi$ system have the same phase (phase coherence).

CP: It explains why the THS moments m = 0,1 are approximately constant as a function of t ($|t| \leq 0.15$ GeV^2). The original purpose of introducing the EBTM was to couple the ρ to a conserved current.[7] Instead of using such an oversimplified model for extrapolation, one uses all or partly the assumptions listed above. In the presence of S and P waves SC is sufficient,[9] for inclusion of higher waves PC is also needed.[10] CM is very convenient because it avoids any extrapolation in t. As shown in Ref. 11 one can use the moments in the region $0.01 \leq t \leq 0.15$ GeV^2. All other analyses use amplitudes with the same spin structure as in the EBTM to extrapolate to the pole. The five recent analyses done on the CERN-MUNICH data are listed in Table I (input data, assumptions, mass range, and type of analysis). All are essentially energy ($m_{\pi\pi}$) independent. Ochs et al.[11] constrained their energy-independent analysis by a K-matrix fit, in order to remove the ambiguities above 1 GeV (see below) and to fix the D-wave below the ρ-mass (essentially the tail of the f meson) which is very poorly determined by the data, as pointed out in Ref. 12. Männer[6] fits several small t and $m_{\pi\pi}$ bins to a parametrization in t and $m_{\pi\pi}$. Both EM and Männer use dispersion relation predictions by Basdevant et al.[14] for the D-wave. All $\pi^\pm\pi^-$ analyses use I = 2 phases which are compatible with a recent determination of Hoogland et al.[15] In a previous publication of EM they showed that apart from the

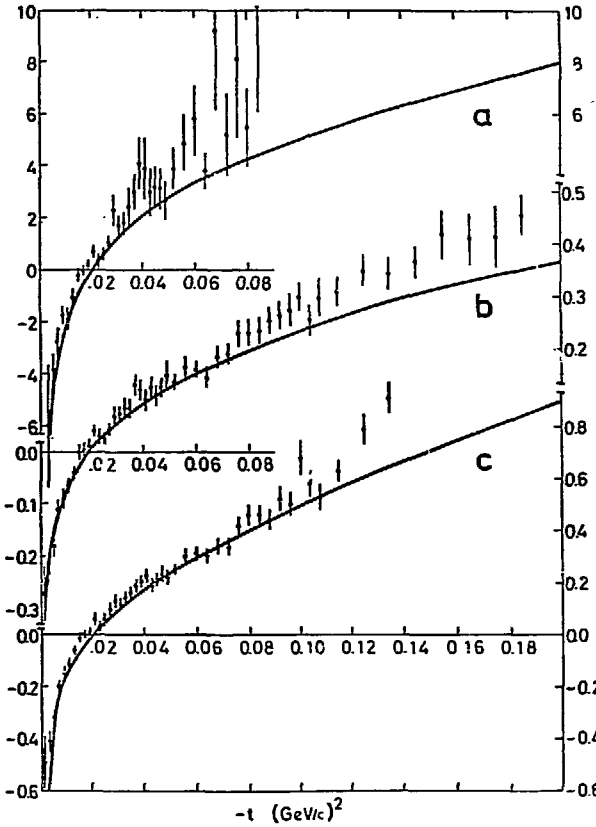

FIG. 3. Ratios of $\pi\pi$ moments as function of t (same data as Fig. 2) in the s-channel helicity system. (a) $-\langle Y_1^2\rangle/\langle Y_2^2\rangle$, (b) $-\langle Y_1^1\rangle$, (c) $\langle Y_1^2\rangle/\langle Y_0^2\rangle$. In all three cases the zero at $t = m_\tau^2$ as predicted by the EBTM (curves) is clearly demonstrated.

TABLE I. Analyses of the CERN - Munich data.

Reference	Input data P_{lab} = (GeV/c)	Assumptions	Range of $m_{\pi\pi}$ (GeV)	Type of analysis
Ochs[11]	17	SC, PC, CM	0.61 - 1.89	EI + K matrix
EM[12]	17	SC	0.51 - 0.97	EI
EM[13]	17	SC, PC, CM	1.02 - 1.78	EI
Männer	17	SC, PC	1.0 - 1.89	EI, over large $m_{\pi\pi}$ and t bins
Männer	7	SC, PC	0.28 - 0.56	EI, over large $m_{\pi\pi}$ and t bins

usual phase-coherent solution, an incoherent solution is also possible,[13] which can be ruled out by comparing the S-wave with $\pi^0\pi^0$ data[13] or results from $\pi^+p \to \pi^+\pi^-\Delta^{++}$ (see below). To compare the results we use for the I = 0 S-wave a nonrelativistic effective range formula

$$\frac{p}{m_\pi} \cot \delta_0^0 = \frac{1}{a_0^0} - \frac{1}{2} r p^2, \qquad (2.7)$$

where p is the $\pi\pi$ center-of-mass momentum. Figure 4 shows that the three groups agree well (a rather unique situation in phase shift analysis), and the simple formula (2.7) fits the data up to the $K\bar{K}$ threshold. For the P-wave we use a relativistic Breit-Wigner formula for the ρ, leading to

$$\frac{p}{\sqrt{s}} \left(\frac{p^2}{\sqrt{s}}\right)^2 \frac{s_0}{p_0^3} \cot \delta_1^1 = \frac{s_0 - s}{\sqrt{s_0}\,\Gamma_0}, \qquad (2.8)$$

where p_0 denotes the value of p at $s = s_0$. The extra factor $1/\sqrt{s}$ on the left-hand side of Eq. (2.8) reflects the fact that $\Gamma(s)$ is a total decay rate and therefore not Lorentz invariant. Again all analyses agree among each other and with (2.8). In principle of 7 GeV/c data are subject to a 15% normalization error which applies simultaneously to the S and P wave. A big change in the normalization would spoil the good agreement between the S and P wave derived from the 17 GeV/c data which are normalized to the unitarity limit of the ρ. The low-energy parameters from the fit are listed in Table II. They pose several difficulties with theory. Both scattering lengths fail the predictions of Weinberg[16] by a factor of 2 to 3. Due to the drastic simplifications entering this calculation, we consider this as not serious. A value of $0.5\ m_\pi^{-1}$ for a_0^0 is compatible with K_{e4}, $\pi^0\pi^0$ [14] and $K \to 2\pi$.[17] Results[18] from an analysis of low-energy πN data with dispersion relations lead to a somewhat smaller value $a_0^0 = 0.12 \pm 0.18\ m_\pi^{-1}$. The very small value of $-0.06 < a_0^0 < 0.03\ m_\pi^{-1}$ obtained from π production data near threshold is based on a misuse of the isobar model.[19] Also, (2.7) has no second sheet pole corresponding to the badly needed ϵ resonance. The data do not rule out a more complicated formula that can contain a distant resonance pole. Nevertheless the *I = 0 S-wave reflects strong attractive forces in this channel.* This strong attraction is denoted by ϵ in the following, independently of whether it corresponds to a resonance or not. The most serious trouble is the value of

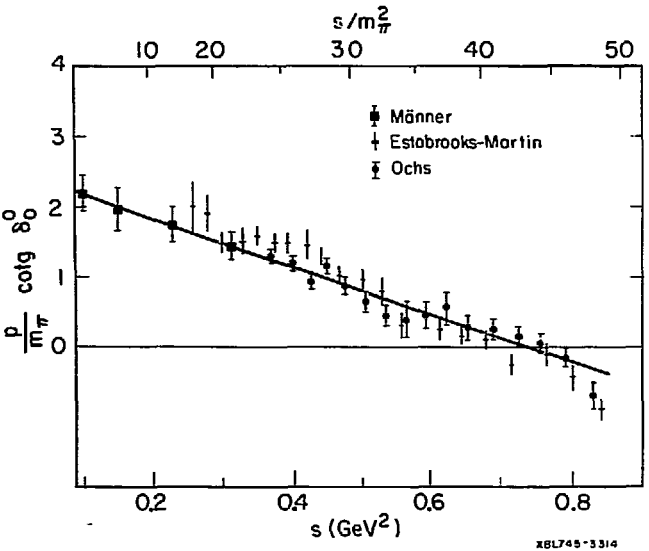

FIG. 4. $I = 0$ $\pi\pi$ S-wave from two analyses done on the 17-GeV/c data [+ = Ref. 12, ● = Ref. 11] and one analysis [■ = Ref. 6] on the 7-GeV/c data from the CERN-Munich group. Plotted is $p/m_\pi \cot \delta_0^0$ as a function of $s = m_{\pi\pi}^2$. The straight line corresponds to a nonrelativistic effective range-formula (see text).

TABLE II. Low-energy parameters for $\pi\pi$ scattering (based on the straight-line fits in Figs. 3 and 4).

	$a_0^0 m_\pi$	$r \cdot m_\pi$	$\sqrt{s_0}$ (MeV)	Γ_0 (MeV)	$a_1^1 m_\pi^3$
Experiment	0.48 ± 0.02[a]	0.53 ± 0.03	779 ± 1	150 ± 10	0.10 ± 0.01
Weinberg[16]	0.17	—	—	—	0.033

[a] Phases of Ref. 6 alone lead to $a_0^0 = (0.44 \pm 0.10) m_\pi^{-1}$.

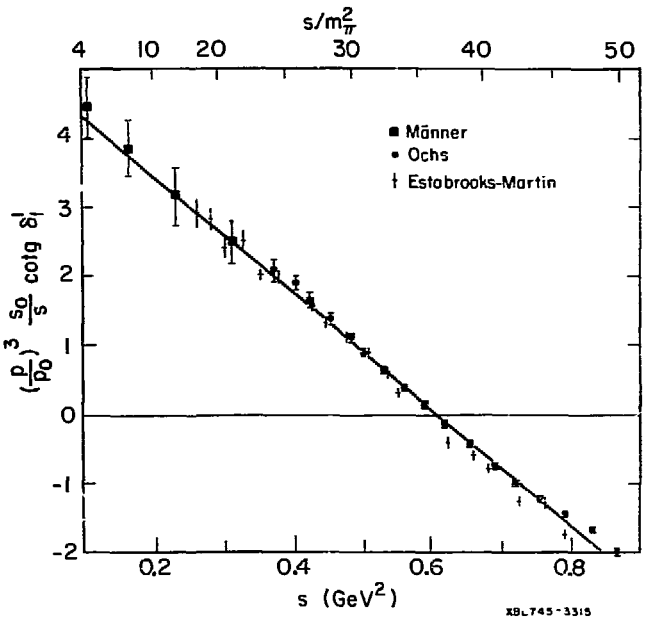

FIG. 5. $(p/p_0)^3$ (s_0/s) cot δ_1^1 for the I = 1 $\pi\pi$ P-wave as function of $s = M^2_{\pi\pi}$ with $\sqrt{s_0}$ = 779 for three different $\pi\pi$ analyses (see Fig. 4). The straight line obtained by a best fit to the points of Ochs and Männer corresponds to a relativistic Breit-Wigner formula for the ρ.

of $a_1^1 = 0.10\ m_\pi^{-3}$. Dispersion relation calculations[14] predict almost the Weinberg value of $0.033\ m_\pi^{-3}$ inside narrow limits. A large value seems to be very hard to accommodate without introducing new singularities (see D. Morgan's minirapporteur's talk).

Preliminary results of a group working with the Ω spectrometer[20] on the reaction $\pi^- p \to \pi^-\pi^+ n$ at 3.2 GeV/c indicate a value of $a_0^0 + \frac{a_0^2}{2} = (0.26\pm0.05)m_\pi^{-1}$ for the $\pi^+\pi^-$ scattering length, closer to the current algebra value. However, they neglect any P-wave and non-OPE contribution in the Chew-Low extrapolation. In view of the puzzling results, we want to remark that all analyses of the CERN-MUNICH data make the assumption of spin coherence for the unnatural exchange amplitudes. Two checks are possible. From SC it follows that the rank of the ππ density matrix cannot exceed 2. In the ρ region positivity allows a determination of the eigenvalues of the density matrix[21] which are shown as a function of $\sqrt{-t}$ in Fig. 6 for the 17-GeV/c data. Only two eigenvalues are significant from zero, as one would expect from SC. If this is not true for smaller $m_{\pi\pi}$ the ππ phases may change. An ultimate check can be only provided by experiments with a polarized target. Another consistency check[22] can be made by using the reaction (2.2). We assume the following simple spin structure of the Δp system (r_p, r_Δ are the helicities of Δ and p):

$$T_{r_p, r_\Delta} = \langle \tfrac{1}{2} r_p\ 1\ r_\Delta - r_p \mid r_\Delta \rangle \cdot \tilde{T}_{r_\Delta - r_p} \quad . \tag{2.9}$$

(2.9) holds in the following cases

1) π-exchange + absorption.[25]
2) Stodolsky-Sakurai for natural exchange.[23]
3) Quark model of Bialas et al.[24]
4) $(\Delta^{++}\bar{p})$ couples to a conserved current.[22]

(2.9) reduces the number of independent amplitudes by a factor 8/3. It can be tested by using the double decay momenta of the ρ and Δ. These predictions are found to be in good agreement with the data.[22] Assuming (2.9), the contribution of the natural exchange can be projected out by the following combinations of Δ-moments:

$$\langle q_{I_+} \rangle = \langle Y_0^0 - \sqrt{5}\, Y_0^2(\Omega_\Delta) - \sqrt{30}\, \mathrm{Re} Y_2^2(\Omega_\Delta) \rangle \quad . \tag{2.10}$$

Knowing the amount of natural exchange to ρ production, the S-wave can be

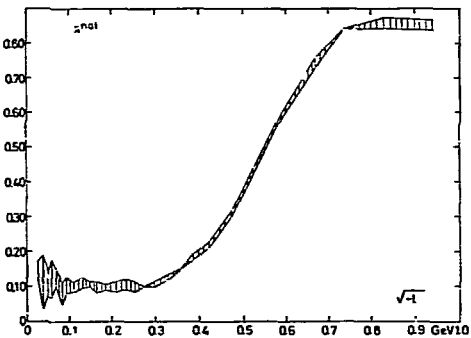

Fig. 9a

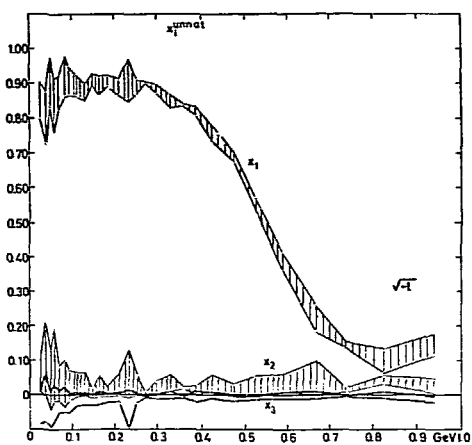

Fig. 9b

XBL 749-1626

FIG. 6. The eigenvalues x of the S-P wave $\pi\pi$ density matrix in the ρ region as a function of $\sqrt{-t}$ (from Ref. 21). If spin coherence is valid, only two can be non-zero.

determined experimentally and compared with the prediction of $\pi^+\pi^-$ phase shifts. The experimental values for the S-wave $\pi^+\pi^-$ cross section are shown in Fig. 7 together with the cross sections calculated from (2.7) and the non-phase-coherent solution of Ref. 13. Clearly the latter can be ruled out by the data. Also the drop in the cross section due to the opening of the $K\bar{K}$ threshold is clearly visible in the data. The agreement of the phases of Ref. 4 with these data and the determination from $\pi^-p \to \pi^+\pi^-n$ supports their method using the extrapolation formula (2.1) without considering any non-OPE background.

Another possible bias results from the poorly known I = 2 phases. Dismissing somewhat deliberately all results from low energy[26] and from deuterium experiments[26] the remaining more recent determinations[15,27] are in reasonable agreement (see Fig. 8) but do not allow any separation between scattering length and effective range formula. The I = 2 phases seem to correspond to a smaller value of a_0^0 which gives another inconsistency for the dispersion relation calculations. In Ref. 28 a large negative I = 2 scattering length is claimed from an experiment at 5 GeV/c on $\pi^+p \to \pi^+\pi^+n$. In view of the apparently large systematic errors in this determination, this result should be treated with caution.

B. $\pi\pi$ above 1 GeV

Above $m_{\pi\pi}$ = 1 GeV $\pi\pi$ becomes inelastic and therefore ambiguities must occur. To fix the unknown overall phase Männer uses the Breit-Wigner resonances f and g; Ochs et al.[11] require the same phase as in the energy-dependent K-matrix fit. EM[13] express their results in moduli and relative phases. Since their finding is very similar to those of Ref. 6, we will not discuss it in detail. The remaining discrete ambiguity can be characterized by the imaginary parts of the zero trajectories[29] in $z = \cos\theta_{\pi\pi}$:

$$T(s,z) = z_0 \prod_{i=1}^{L} [z - z_i(s)] . \qquad (2.11)$$

If only $|T|^2$ is measured, $z_i \to z_i^{\pm}$ leads to a 2^L ambiguity for L + 1 partial waves. Continuity in energy requires that a transition from one solution to another can occur only where Im $z_i(s) = 0$. Since the interference of the OPE with the background is also measured, this treatment of the ambiguity is not quite correct. One has to reflect Im $z_i(s)$ and perform a new fit to the data. A plot[6] of Im $z_i(s)$ as function of $\sqrt{s} = m_{\pi\pi}$ is shown in Fig. 9. The solutions compatible with unitarity can be labelled by the values of Im z_i at

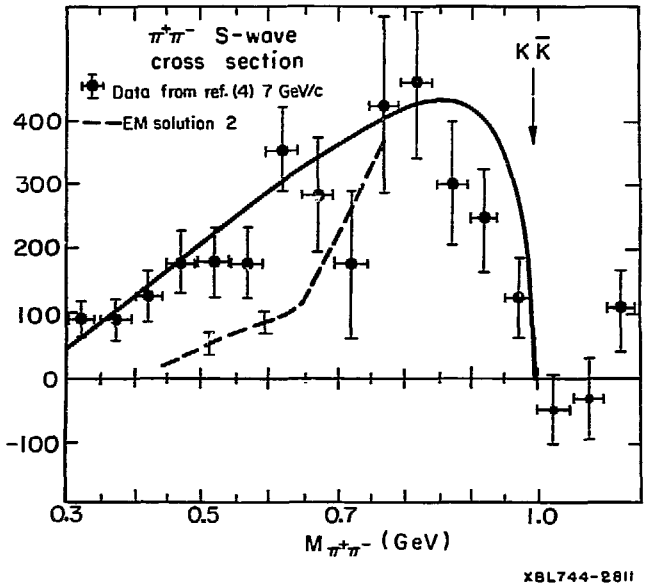

FIG. 7. $\pi\pi$ S-wave cross section (Ref. 22) from the reaction $\pi^+p \to \pi^+\pi^-\Delta^{++}$ at 7 GeV/c as function of $M_{\pi\pi}$ ($0 < |t'| < 0.4$ GeV^2). The solid line is based on the phases of Ref. 11 and the assumption of π-exchange. The dashed line corresponds to the phase-incoherent solution of Ref. 12a, which is ruled out by the data.

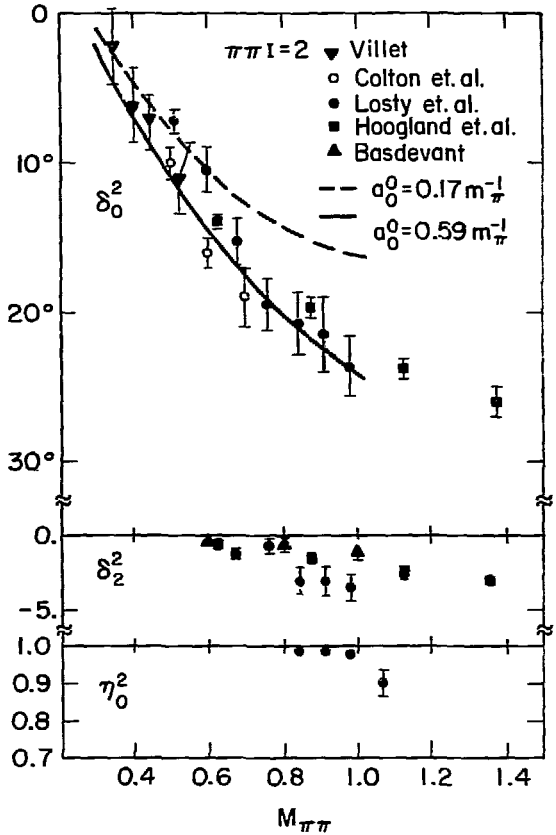

XBL 745-3177

FIG. 8. I = 2 ππ phase shifts as function of ππ mass. The points ▼, O, ●, ■ are the result of phase shift analysis of Refs. 27 and 15, ▲ the D-wave prediction of the theoretical calculation of Ref. 14, and the curves are S-wave predictions of Ref. 14 labelled by the value of the I = 0 scattering length.

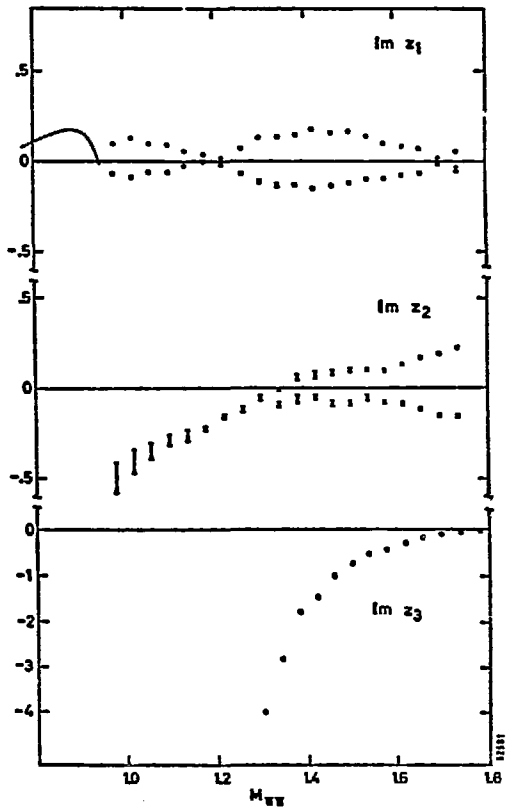

FIG. 9. The imaginary part of the zero trajectories $z_i(m_{\pi\pi})$ as function of $m_{\pi\pi}$ from the analysis of Ref. 6. Due to the interference of the OPE term with the background the symmetry $\mathrm{Im}\, z_{1,2} \rightarrow -\mathrm{Im}\, z_{1,2}$ is only approximately true.

$m_{\pi\pi} \approx 1.5$ GeV. Since they are published,[6] we present two extreme cases (--- and ++-) for the S(P) wave in Fig. 10(11). Solution (---) shows no structure at all. Both EM and Manner slightly favor this solution, without being able to rule out the (++-) solution which shows an even stronger ρ' solution. Frogatt et al.[30] showed that the solution of Ochs does not average any reasonable Regge amplitude as duality requires. For improvement they take $|T|^2$ reconstructed from the phase of Ref. 11 (ignoring the additional experimental information from background OPE interference) together with fixed t dispersion relations to determine a new phase. This method has been successfully applied by Piettarinen[31] in πN scattering. The new solution now satisfies duality. Their P-wave is indicated by the dashed line in Fig. 11, which clearly favors the (++-) solution of Ref. 6, leading to a nice ρ' signal.

If we take this as an argument for the existence of the ρ', still its width caused some confusion. In Table III various determinations[32-34] are collected together with my own fit to the phases of Ref. 11, which takes into account the phase space factor in the total width due to the dominant $\epsilon\rho$ decay mode.[33] One sees that $\Gamma_{\rho'}$ depends largely on one's prejudice about the background and the resonance form. Also the new solutions of Ref. 6 will add four more columns.

An experimental decision about the existence of ρ' can be provided by accurate data on $\pi^- p \to \pi^0\pi^0 n$. As Fig. 10 shows, the S-wave is very different for the various solutions. Present data do not allow making any conclusion.

Another way to study mesons in this region is to look at their $K\bar{K}$ mode. Measuring $\pi^- p \to K_S K_S n$, one can extract $\pi\pi \to K\bar{K}$ amplitudes under assumption of dominant π-exchange. From the known $\pi\pi \to \pi\pi$ phases and two-channel unitarity one can obtain $\delta(K\bar{K} \to K\bar{K})$ for the I = 0 S-wave. This has been done by Beusch et al.[35] with their data at 9 GeV/c. The up-down ambiguity leads to two solutions, one showing a rapid energy variation in the f-region, the other favors a large negative scattering length in $K\bar{K}$, to be expected from the S^* as a virtual bound state (see Fig. 12).

At this conference, data on $\bar{p}p \to K^0_S K^0_S \pi^+\pi^-$ in the region of $P_{lab} = 0.7$-0.75 GeV/c have been presented.[36] They found an enhancement at threshold in the $K^0_S K^0_S$ mass spectrum that one would expect from the phases of Ref. 4. Present data are not sufficient to distinguish between a resonance and a virtual bound state. The result of any of those fits depends on the parametrization one starts with. The resonance parameters together with earlier determinations are listed in Table IV.

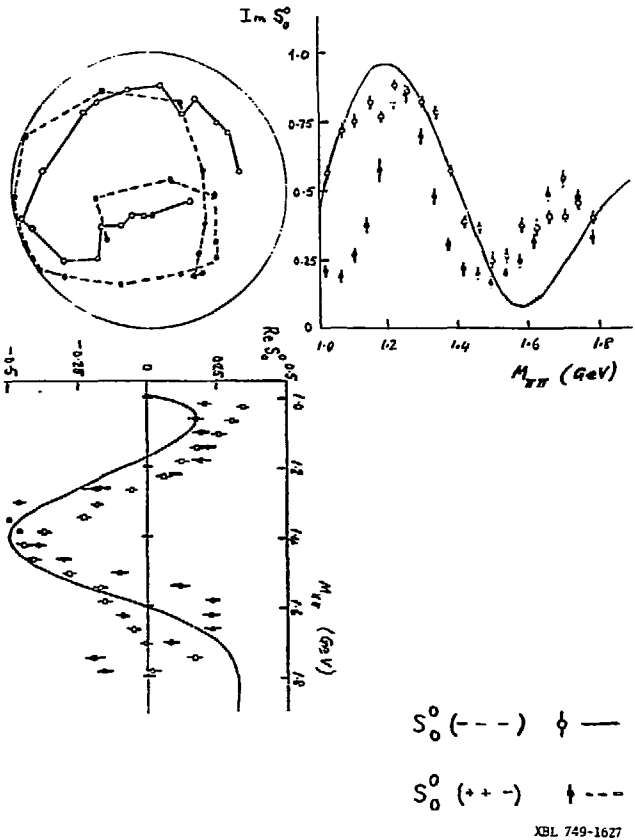

FIG. 10. Real part and imaginary part of the I = 0 ππ S-wave as function of $m_{\pi\pi}$ for two solutions [o (---) and ● (++-)] of Ref. 6 and for the K-matrix fit of Ref. 11. In the Argand diagram only the two solutions of Ref. 6 are shown [(---) is indicated by a solid line and (++-) is indicated by a dashed line].

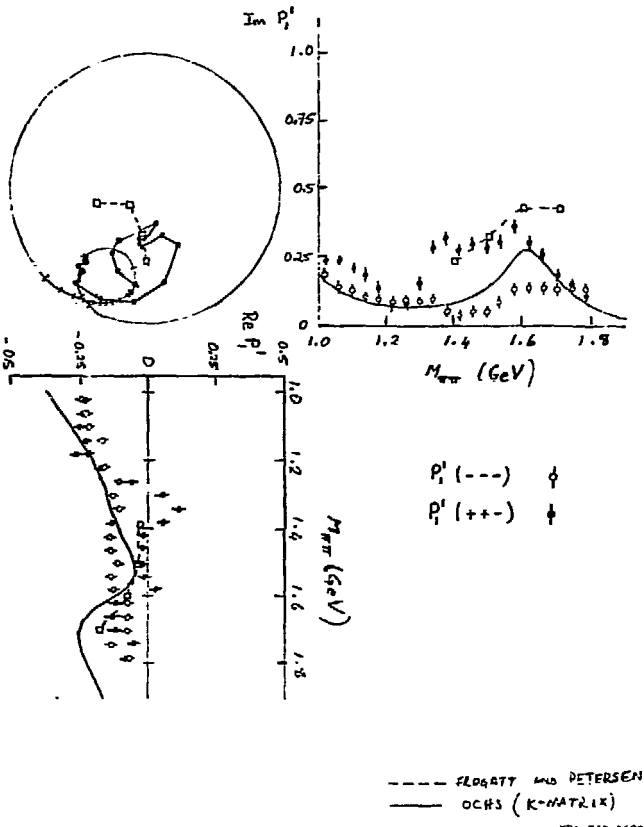

FIG. 11. Same as Fig. 10 for the I = 1 P-wave. The (++-) solution (indicated by ● and -●- in the Argand plot) shows a ρ' signal, whereas the (---) solution shows no resonance at all (indicated by ○, not shown in the Argand plot). The dispersion relation calculation of Ref. 30 (---□---) favors a solution of type (++-).

TABLE III. ρ' parameters

	A (Ref. 11)	B	C (Ref. 32)	D (Ref. 33)	E (Ref. 34)
X	0.25 ± 0.05	0.23 ± 0.05	0.248 ± 0.014	< 0.20	—
$m_{\rho'}$	1590 ± 50	1650 ± 50	1617 ± 5	1540	1600 ± 150
$\Gamma_{\rho'}$	180 ± 50	250 ± 50	420 ± 20	> 350	broad

TABLE IV. $S^{\pm}$ parameters

Ref. →	36	4	11	91	92
M	1040 ± 4	997 ± 6	1007 ± 20	987 ± 6	1012 ± 6
Γ	52 ± 10	54 ± 16	30 ± 10	52 ± 12	34 ± 10

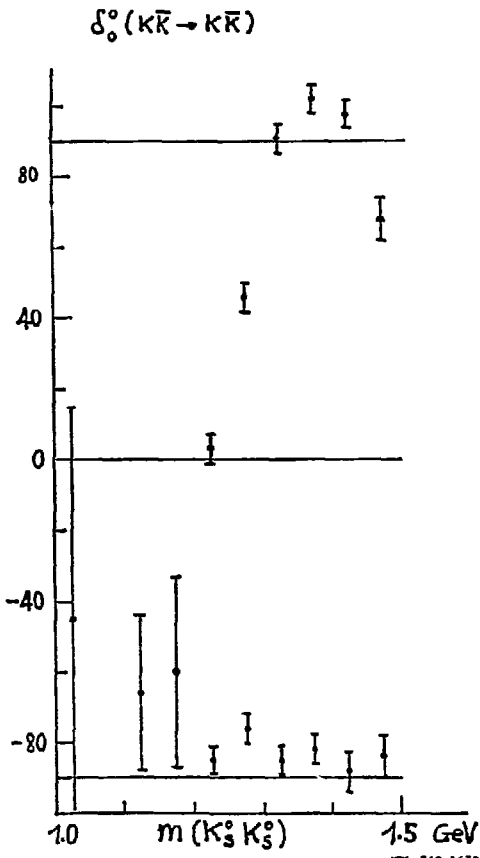

FIG. 12. $K\bar{K} \to K\bar{K}$ S-wave phases from Ref. 35 as a function of the KK-mass. Above 1.2 GeV there are two solutions corresponding to the up-down ambiguity above the f-meson.

The decay of mesons into K^+K^- has been studied by the CERN-MUNICH group[6] and the EMS group at Argonne.[37] Figure 13 shows the mass spectrum from preliminary data[6] at 18.8 GeV/c for $|t| \leq 0.25$ GeV^2. The threshold enhancement produced by the S^* effect, the interfering A_2 and f meson, and the g meson are clearly visible. In the 2-GeV region the N $\langle Y_0^8 \rangle$ distribution shows (Fig. 14) an enhancement around 2 GeV mass. The N $\langle Y_0^7 \rangle$ moment shows approximately the pattern one expects from an interference between the g meson and a new $l = 4$ meson with M = 2 GeV and Γ = 250 MeV. Additional support for this interpretation comes from an experiment at the CERN Ω spectrometer[38] measuring $\pi^- p \to \pi^- \pi^+ n$ at 12 GeV/c. The $\pi\pi$ moments (uncorrected for acceptance) are shown in Fig. 15, which indicates additional structure above the g meson due to the l =4 wave. Before establishing that this is a resonance, one has to wait for phase shift analysis to be done on these data.

C. Kπ Scattering

The low-energy Kπ system is easier to analyze than $\pi\pi$, because the D-wave is negligible and the $K^*(890)$ is relatively narrower. Using the pole extrapolation, Matison et al.[38a] resolved the up-down ambiguity for the S-wave above the $K^*(890)$ in favor of the down solution (no narrow κ unless $\Gamma_\kappa < 7$ MeV) by studying the reaction

$$K^+ p \to K^+ \pi^- \Delta^{++}. \qquad (2.12)$$

To check on the influence of non-OPE background in this reaction, we can do the same analysis as for the π reaction (2.2) by using the Δ^{++} moments to separate off the S-wave cross section.[22] The comparison of this analysis of the data of Ref. 38a with the prediction of their Kπ phases is shown in Fig. 16. Both agree reasonably well; therefore, the non-OPE background does not affect the extrapolation too much. Above 1 GeV, results from the SLAC spectrometer[39] are presented at this conference for reaction (2.12) and the reaction

$$K^- p \to K^- \pi^+ n. \qquad (2.13)$$

Figure 17 shows the Kπ moments as a function of the Kπ mass. Both $K^*(890)$ and $K^*(1400)$ are sitting on a large background. From the ratio of this background in the N$\langle Y_0^2 \rangle$ and N$\langle Y_0^0 \rangle$ distributions, one concludes that the background must be mainly S-wave (resp. SD wave interference). From the absence of any structure in the N$\langle Y_0^6 \rangle$ moments near 1400 MeV one can eliminate the possible 3^- assignment for the $K^*(1400)$ listed in the PDG tables.[40] In Fig. 18 the moments

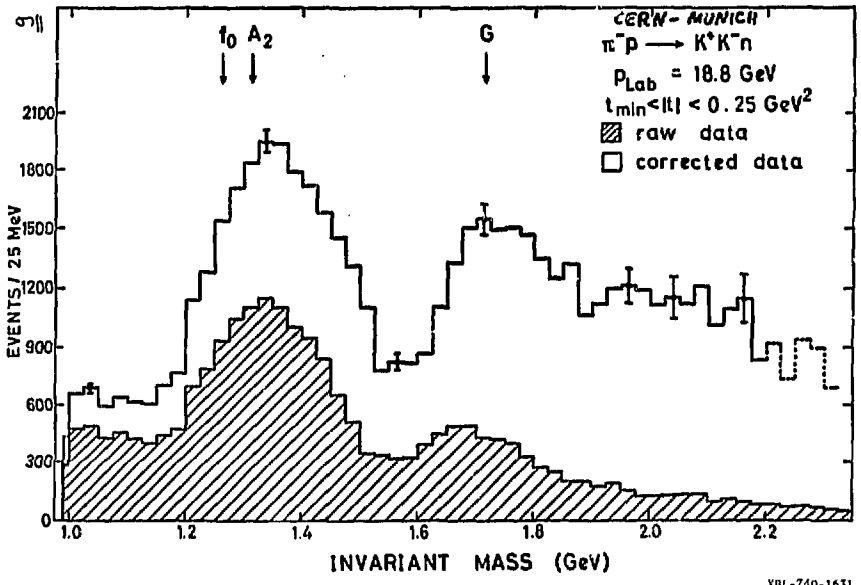

FIG. 13. K^+K^- mass distribution from Ref. 6 at small $|t|$.

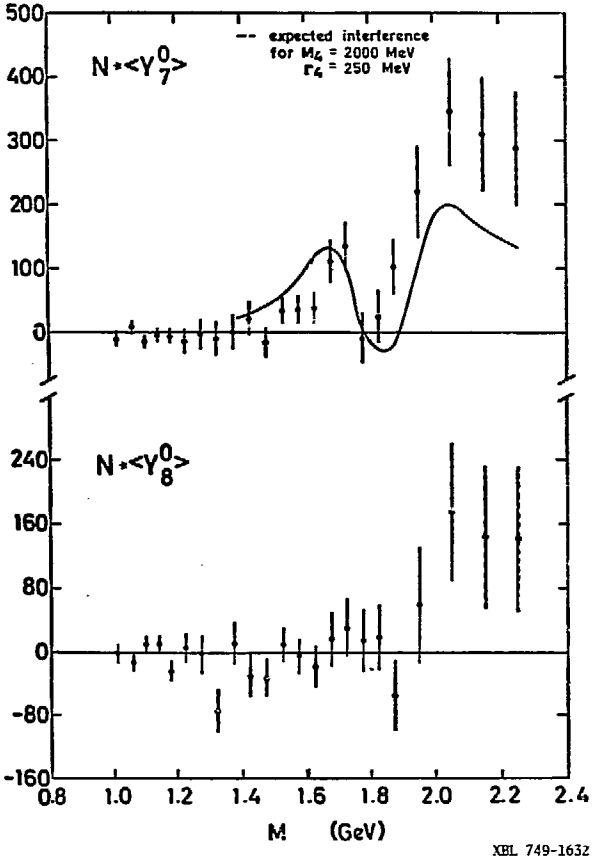

FIG. 14. Unnormalized moments $N\langle Y_L^0 \rangle$ for L = 7,8 as a function of $M_{K\overline{K}}$ from the reaction $\pi^- p \to K^+ K^- n$ at 18.8 GeV/c.[6] The curve corresponds to what is expected from the interference of f(2000) $\to K^+K^-$ with ($J^P = 4^+$) with the g meson ($J^P = 3^-$).

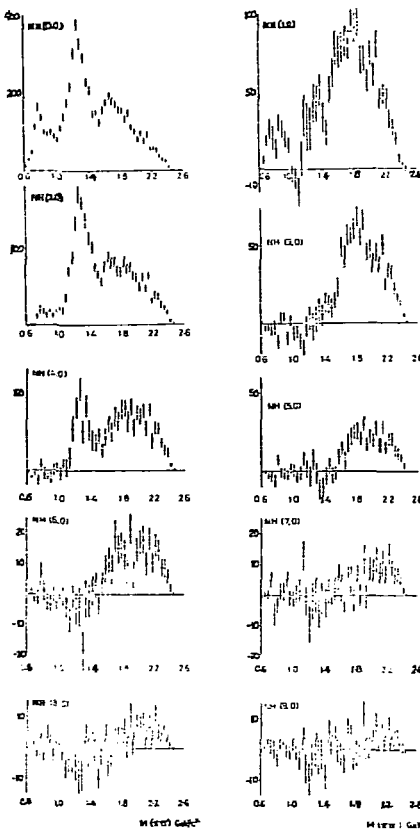

FIG. 15. Unnormalized $\pi\pi$ THS moments of Ref. 38, $NH(L,M) = \sqrt{4\pi/2L+1}\ N\langle Y_M^L \rangle$ as a function of $M_{\pi\pi}$ (not corrected for acceptance) from the reaction $\pi^- p \to \pi^- \pi^+ n$ at 12 GeV/c.

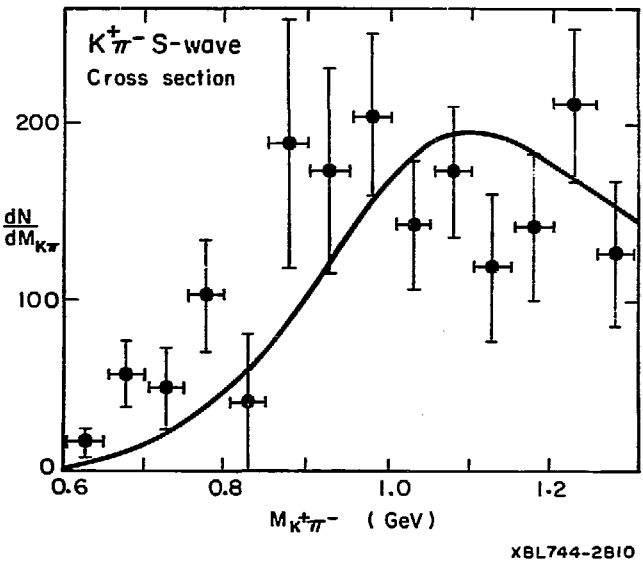

FIG. 16. $K^+\pi^-$ S-wave cross section (●) from the reaction $K^+p \to \pi^-\Delta^{++}$ at 12 GeV/c[22] for $|t| < 0.4$ GeV^2 using the Δ^{++} decay moments to separate natural exchange and unnatural exchange contribution to the Kπ P-wave. The curve gives the OPE prediction of the analysis of Ref. 38a.

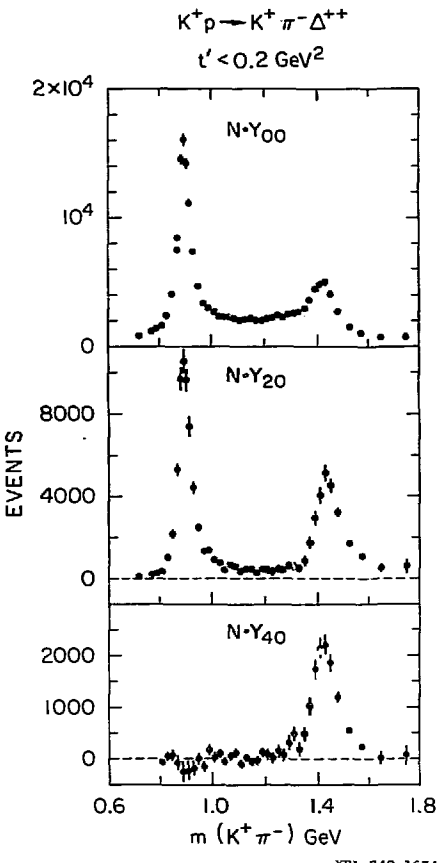

FIG. 17. Unnormalized Kπ moments[39] from the reaction $K^+p \rightarrow K^+\pi^-\Delta^{++}$ at 13 GeV/c ($|t'| < 0.2$ GeV^2).

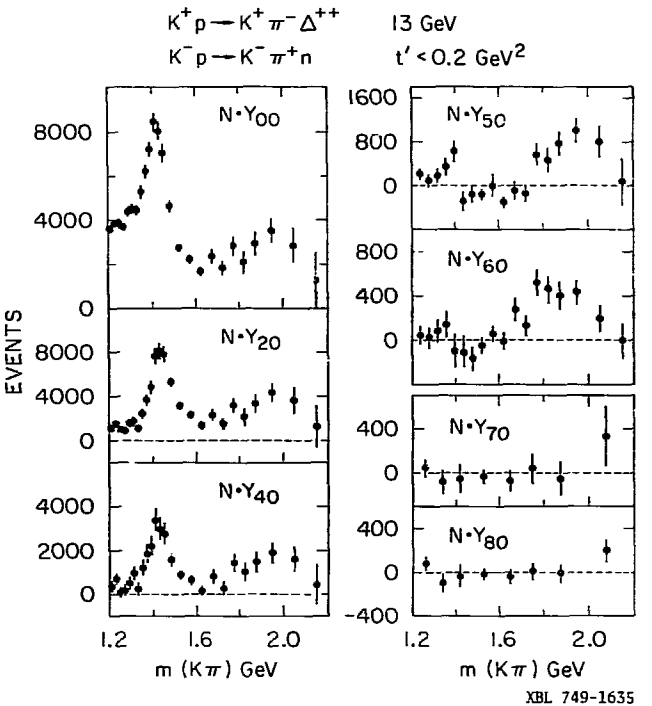

FIG. 18. Unnormalized Kπ moments[39] from the combined reactions $K^+p \to K^+\pi^-\Delta^{++}$ and $K^-p \to K^-\pi^+n$ at 13 GeV/c. The high moments show evidence for a 3^- $K^*(1800)$.

in the higher mass region [both reactions (2.12) and (2.13) combined] are shown. A broad bump around 1800 MeV is seen in all even moments $N\langle Y_0^L\rangle$ up to L = 6. The L = 5 moment shows the interference pattern one expects from an interference of the $2^+K^*(1400)$ with a 3^-K^* with mass 1800-1850 MeV and a width of 200 MeV. This bump has been observed earlier,[41] but the statistics of these experiments did not allow a determination of the spin. A large S-wave under the $K^*(1400)$ has also been reported[42] from an analysis of reaction (2.13) at 10 and 16 GeV/c. Parameterizing their result as a non-relativistic Breit-Wigner resonance (equivalent to Eq. 2.7),

$$\frac{p}{p_0}\cot\delta = \frac{m_0^2 - S}{m_0\Gamma_0},$$

they find the values of $m_0 = 1245 \pm 30$ MeV and $\Gamma_0 = 485 \pm 80$ MeV. This just says that one has a strong S-wave interaction, but by no means a resonance. Similar results have been found earlier by Cords et al.[42a] yielding values of $m_0 = 1305 \pm 30$ and $\Gamma_0 = 330 \pm 60$ MeV. A big difference between πN and $\pi\pi$ or $K\pi$ analyses is lack of information on total cross section in the latter case. In principle one can measure, for example, $\sigma_t(\pi^+\pi^-)$ in the reaction

$$\pi^+ p \to \Delta^{++} + \text{anything}$$

by the Chew-Low extrapolation. Attempts have been made[43] ignoring other exchanges than π. However, the assumption (2.9) on the Δp coupling enables one to separate the contribution of the high-lying natural trajectories $\rho, A_2 \cdots$. This is a definitive advantage of Δ^{++} inclusive over n inclusive reactions. Inclusive experiments with measured Δ^{--} would be of great help in the high-mass $\pi\pi$ or $K\pi$ region.

III. MESONS SEEN IN 3π AND $K\pi\pi$ DECAY MODE

The key word in this field is the so-called Illinois partial wave analysis program by Ascoli and his disciples.[44,45] How well Ascoli did his job one can see from the fact that not only his method but also his program is used by all analyses except one.[46] The amplitude for a reaction like

$$\pi N \to \pi_1\pi_2\pi_3 N \qquad (3.1)$$

is expanded in quasi-two-body states $\rho_{12}\pi_3$, $\rho_{13}\pi_2$, $\epsilon_{12}\pi_3$, $f_{12}\pi_3 \cdots$, where $\rho_{ik}\pi$, $f_{ik}\pi$, $\cdots$ stand for P, D, $\cdots$ wave interaction between π_i and π_k. For K induced reactions

$$KN \to K_1 \pi_2 \pi_3 N \qquad (3.2)$$

one has both sequences ϵK, ρK, fK and $\pi\kappa$, $\pi K^{*}(890)$. The amplitude for the process (3.1) is then expanded into partial waves

$$T(3\pi) = \sum_{\substack{\text{PERM} \\ ik \\ K}} D^{K}(\Omega_{3\pi}) \; R(s_{ik}) \; T^{K}, \qquad (3.3)$$

where D describes the dependence on the three Euler angles of the 3π system usually with respect to the incoming π direction (THS), K abbreviates the total spin J, helicity r, decay system $\rho\pi$, $\epsilon\pi$, $\cdots$ and parity. $R(s_{ik})$ contains the phases describing the $\pi_i\pi_k$ subsystem and T^{K} are the amplitudes for producing the 3π system. Finally one has to sum over all K and the three possible permutations of $\pi_1 \pi_2 \pi_3$. For reaction (3.1) this is necessary to satisfy Pauli's principle. Still (3.3) is the most general expansion. Assumptions come in by the so-called isobar model:[45]

(i) One restricts J to values less than 2 or 3, depending on the total mass $M_{3\pi}$ of the 3π system and neglects all contributions where π_i, π_k are in an exotic state. Experimentally there is no need to include helicities $|r| > 1$ in the THS. Therefore only amplitudes T^{k} with $|r| \leq 1$ are considered.

(ii) In general T^{K} depends on the total energy s, momentum transfer t, and the Dalitz plot variables. Factorization implies that T depends only on the production variables $s, M_{3\pi}$, and t.

Due to limited statistics many additional assumptions have to be made as to phase coherence (all amplitudes with the same J are relatively real), spin coherence (only no flip at the nucleon vertex), etc. All analyses perform maximum-likelihood fits to include cuts for N^{*} production and acceptance corrections. There are two ways to perform the fit. The $\pi^{+}p \to \pi^{+}\pi^{+}\pi^{-}p$ analysis at 7 GeV/c of Ref. 46 uses the amplitudes as fitting parameters, whereas all others use the 3π density matrix,[42,44,47-51]

$$\rho^{K\overline{K}} = \sum_{\substack{\text{nucleon} \\ \text{spins}}} T^{K}(T^{\overline{K}})^{*}. \qquad (3.2)$$

This choice has the advantage of a unique solution. However, one has to worry about the rank condition ($\text{Rg}\rho \leq 4$). Using the amplitudes this is built in, but then one has to fight against the ambiguity problem, as for any partial wave analysis. For low values of J both are equivalent. Since most of the

results on 3π are known I will discuss only a few topics which are new and/or have impact on the existence (or nonexistence) of resonances. The only established resonances are $A_2(1300)$ in 3π and the $K^{\pm}(1400)$ in Kππ. A split A_2 is now conclusively ruled out by a BNL experiment[52] with more than 10 standard deviations in the reaction $\pi^- p \to K^0 K^- p$ at 23 GeV/c. At the last conference C. Michael[53] concluded on the basis of private communications that the energy dependence of the production cross section of A_2 decaying into K^0K^- drops faster than s^{-n} with n = 0.5, as seen in its ρπ decay.[42,44,47] My version of private communications of CERN results[54] are shown in Fig. 19. $\sigma(A_2 \to \rho\pi^-)$ has the same energy dependence as $\sigma(A_2 \to K^-K^0)$. Since the ratio A_2 to A_1 or A_3 production is independent of the energy, A_2 must have a substantial coupling to P exchange in addition to ρ and f. Support for P and f coupling comes from an experiment on 3π production on nuclei.[50] Figure 20 shows that both 1^+ and $2^+(A_2)$ cross section in the region $1.2 \leq M_{3\pi} \leq 1.4$ have the sharp increase at small t due to coherent production. A_2 is suppressed since $\frac{d\sigma}{dt}(A_2)$ must vanish at t = 0 because of parity conservation. This explains why A_2 has not been seen in bubble chamber experiments on coherent production of deuterium.[51,55] From that we conclude that ρ exchange (dominant spin flip) cannot be large. To check this we consider the charge exchange reaction $\pi^+ p \to \pi^+\pi^-\pi^0\Delta^{++}$.[56] The 3π mass spectrum at 7 GeV/c is shown in Fig. 21. Using the coupling (2.9) for the $\Delta^{++}p$ vertex, we can separate natural exchange (shaded area). There is hardly any A_2 signal left, which means A_2^0 must mainly be produced by B exchange and not by ρ. The suppression of ρ exchange in the A_2 production has been predicted theoretically by Hoyer et al.[57] and G. Fox et al.[1]

Now we turn to A_1 production, the peak of 1^+ S (ρπ) wave near $M_{3\pi} = 1100$ MeV. As shown by Ascoli et al.[58] the main features can be accounted for by the Deck model. Especially the prediction of the relative phases between the various amplitudes are in surprisingly good agreement with experiment. The relative amount of P and f exchange for A_2 production can be obtained by a Regge fit to $\sigma(A_2)$ (solid line in Fig. 19). Adding the A_1 Deck model to A_2 production, one can predict the relative production phase[52] between the A_1 and A_2, shown in Fig. 22 as a function of P_{lab} for various t intervals in agreement with the experimental data. Another striking feature is the correct prediction of the relative phase of ~ 90° between the $1^+P(\epsilon\pi)$ and the $1^+S(\rho\pi)$ waves in the A_1 region.[58] The mass spectra for the 1^+ S (ρπ) and

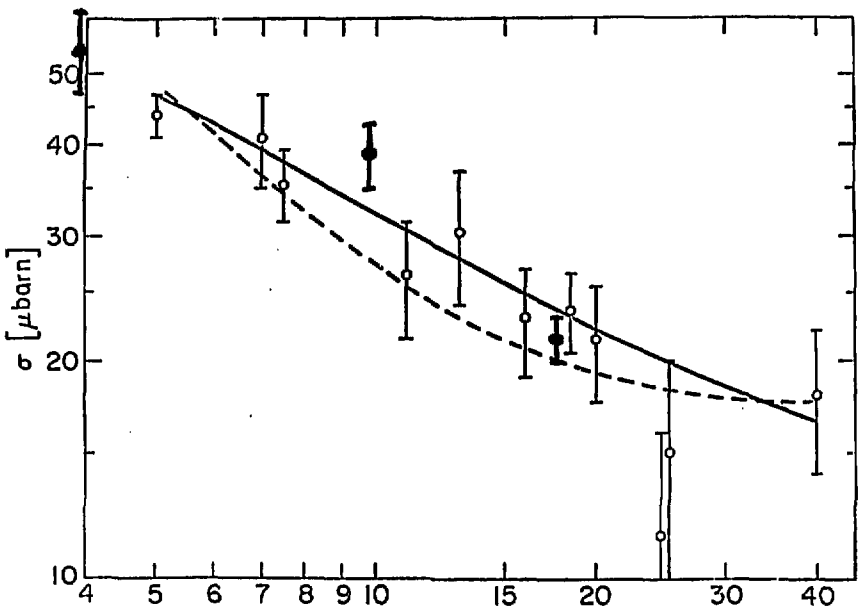

FIG. 19. A_2 natural exchange production cross section for $|t'| < 0.8$ GeV^2 as a function of the laboratory momentum (A_2 is defined as the 2^+ wave in the mass range $1.2 < M_{3\pi} < 1.4$). ϕ denote the cross section of $\sigma[\pi^- p \ (A_2 \ \pi^{3\pi} p)p]$ from Ref. 59; $\blacklozenge$, $\blacktriangle$ - the values of $6.8 \cdot \sigma[\pi^- p \to (A_2 \to K^- K^0)p]$ of Ref. 54. The curves correspond to a Regge fit using P and f exchange.[59]

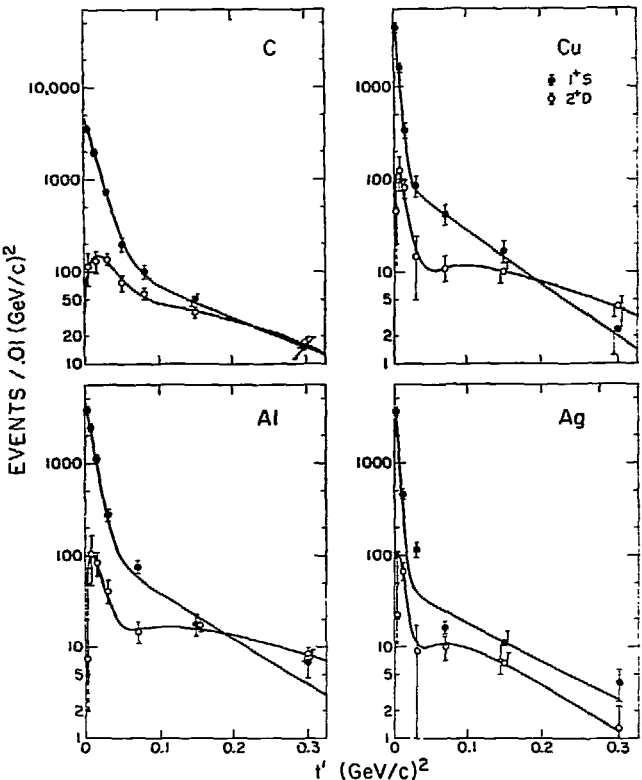

FIG. 20. Contribution of the 1^+S and 2^+D states to the $\pi A \to 3\pi A'$ cross section at 23 GeV/c from Ref. 50 in the mass range $1.2 < M_{3\pi} < 1.4$ GeV as a function of t'. The curves are fits of the form $e^{Bt'}$ (for 1^+) and $|t'|e^{Bt'}$ (for 2^+).

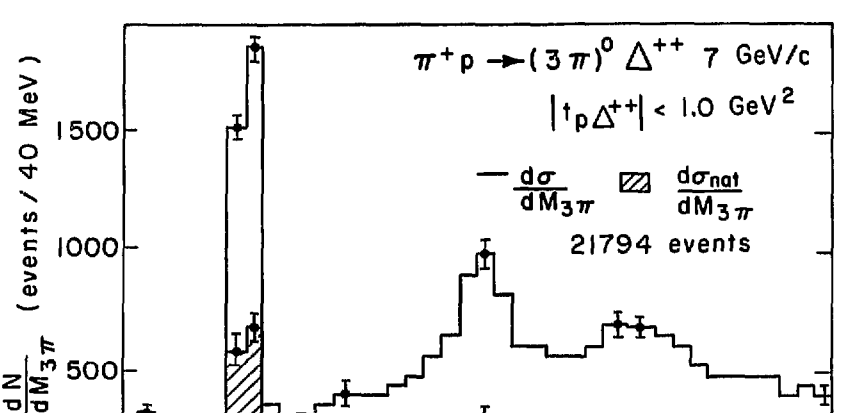

XBL745-3320

FIG. 21. $\pi^+\pi^-\pi^0$ mass spectrum from the reaction $\pi^+ p \rightarrow (3\pi)^0 \Delta^{++}$ at 7 GeV/c from Ref. 56. The absence of any A_2 signal in the natural exchange cross section (hatched histogram) means that A_2^0 is mainly produced by unnatural exchange (B).

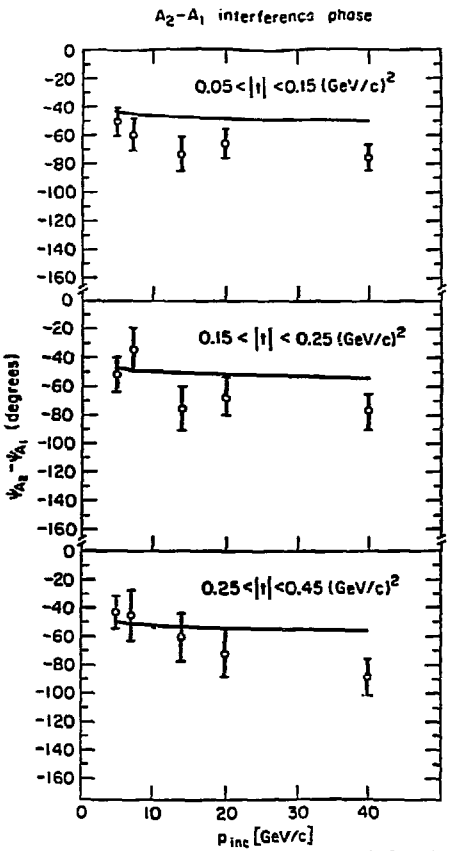

FIG. 22. Interference phase between the A_1 and A_2 production amplitudes as a function of the laboratory momentum at various $|t|$. ϕ = result of the analysis of Refs. 44 and 47, and the curve is the prediction of the Deck model for A_1 and a P-f Regge fit for A_2 (taken from Ref. 59).

2^+D ($\rho\pi$) waves are shown in Fig. 23 together with the relative phase to the 0^- wave from Ref. 46. A_2 shows the phase variation as expected for a B.W. resonance, whereas A_1 shows for $|t| \leq 0.1$ GeV^2 no significant phase variation. Also the peak moves going to the $|t|$-interval $0.1 \leq |t| \leq 0.6$ GeV^2. All this makes a resonant interpretation very doubtful. Bowler[60] proposed a model of a superposition of a diffractively produced resonance and a background picking up the resonance phase by final state interaction. By appropriately chosen coefficients this leads, as he says, to an almost constant phase in the total amplitude and to a reasonable fit to the A_1 line shape of Ref. 47. He predicts the mass of the A_1 to be about 1300 MeV. This rather artificial resonance interpretation of the A_1 is mainly motivated by the need of the quark model for 1^+ states. Clearly analysis of charge-exchange data will be able to make the decision, if it is not done already (see Fig. 21). In their 6 GeV/c π^+d data S. Dado et al.[61] found in the final state $\pi^+K^+K^-$d an enhancement around 1575 MeV in the $\pi K\overline{K}$ mass distribution. They identify this bump with the $E_1(1540)$ meson. The decay distributions are compatible with 2^- and 1^+. 1^+ and the observed dominant $K^{\pm}\pi$ decay would allow a Deck-type interpretation.

Another problematic state is the A_3 bump [2^- S ($f\pi$)] around 1700 MeV. Figure 24 shows the phase of this wave relative to 0^- as function of $M_{3\pi}$. Experiments with π^+ [48,49] seem to favor a phase variation, whereas π^- experiments[44,47] do not. Since $N^{\pm}$ pollution may affect the angular distribution in experiments with lower beam momentum, we have to wait for further experiments at high energies and better statistics before claiming any effect.

The results on $K\pi\pi$ are much less conclusive, because the system is more complicated and usually much fewer statistics are available. In addition one has in the non-charge-exchange reaction K and π with equal charge. In the Q bump roughly 25% of all events allow also a fit with interchanged K and π. This is precisely the region where one can distinguish $K\rho$ and $K^{\pm}\pi$ final states. In a study[49] of the reaction $\pi^+p \to \pi^+\pi^-\pi^+p$ at 8, 10, 23 GeV/c and $K^-p \to K^-\pi^-\pi^+p$, $K^0\pi^+\pi^-n$ at 8, 10, 16 GeV/c[62,63] the (3π) and the two K reactions have been compared. Their results are quoted in Table V which gives the fraction of unnatural states (0^-, 1^+), natural exchange, resonance production in 2^+, the mass interval, and the exponent in $\sigma \sim P_{lab}^{-n}$. Obviously the $(3\pi)_{\Delta Q = 0}$ and $(K\pi\pi)_{\Delta Q=0}$ behave very similarly, but also $(K\pi\pi)_{\Delta Q=1}$ has a large fraction of natural exchange in contrast to what we saw before the $(3\pi)_{\Delta Q=1}$ Δ^{++} reaction.

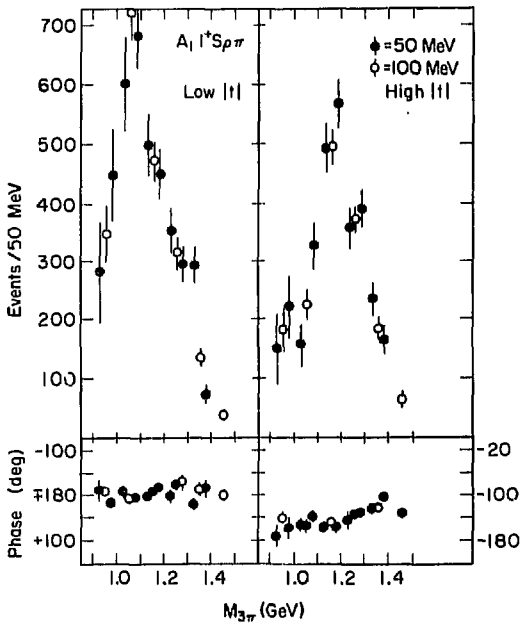

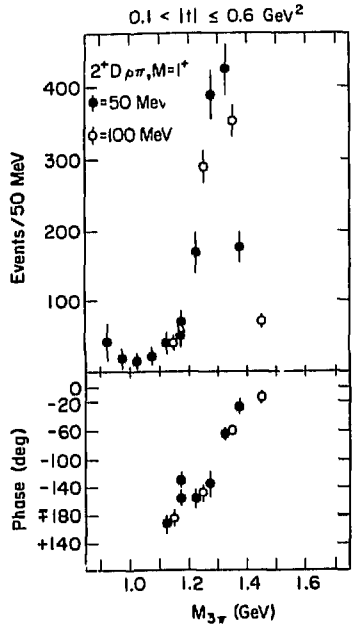

FIG. 23. Intensity and relative phase against 0^- for A_1 and A_2 as a function of $M_{3\pi}$. Both are given for 50- (●) and 100-MeV (◇) mass bins. The A_1 cross sections are shown for two t intervals (low $|t|$: $|t| < 0.1\ GeV^2$, high $|t|$: $0.1 < |t| < 0.6\ GeV^2$).

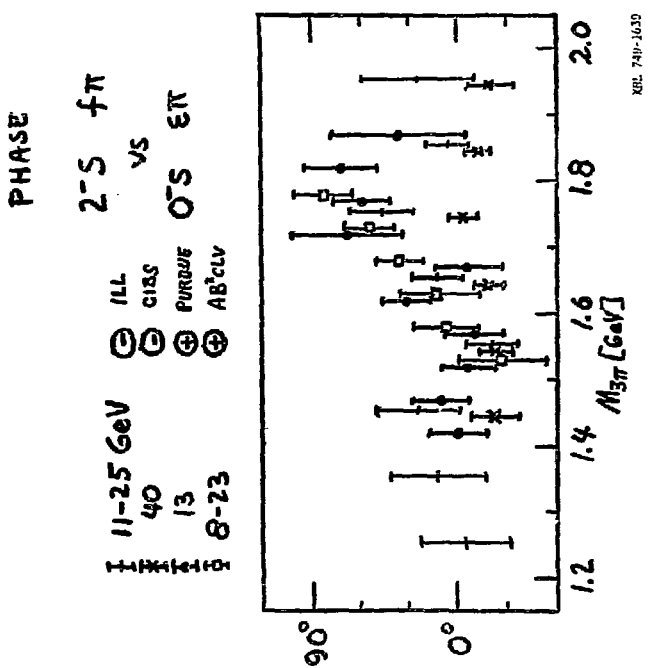

FIG. 24. Phase between the $2^-S(f\pi)$ wave (A_3) and $0^-S(\epsilon\pi)$ wave as a function of 3π mass. [+ = π^-p 11-25 GeV/c,[44] × = π^-p 40 GeV/c,[47] ● = π^+p 13 GeV/c,[48] ⊕ = π^+p 8-23 GeV/c.][49]

TABLE V. Contribution to the $(3\pi)_{\Delta Q = 0}$ and $(K\pi\pi)_{\Delta Q = 0,1}$ cross section for $\pi^+ p \to \pi^+\pi^+\pi^- p$[49] and $Kp \to K\pi\pi N$.[62,63]

	Unnatural spin parity (3π) states	Natural exchange	$2^{\pm}$ resonance contribution	Mass interval	Exponent n in $\sigma \propto P_{lab}^{-n}$
$(\pi\pi\pi)_{\Delta Q = 0}$	~90%	~100%	~10%	0.8-2.0	~0.5
$(K\pi\pi)_{\Delta Q = 0}$	~90%	~95%	~10%	1.0-2.1	
$(K\pi\pi)_{\Delta Q = 1}$	~65%	~80%	~35%	1.04-1.56	1.5-2

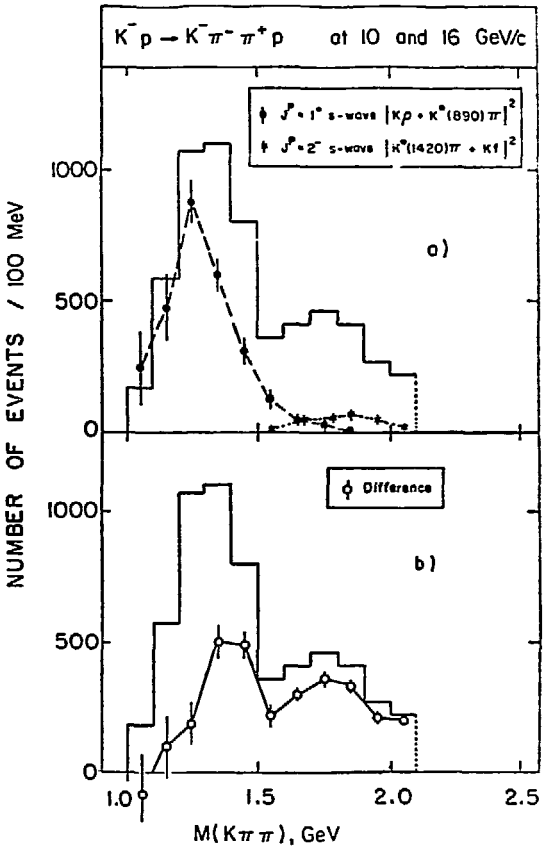

XBL 749-1640

FIG. 25. a) Comparison of the experimental Kππ mass spectrum (solid line) with the contributions of 1^+ S[K* π + Kρ] (●) and 2^- S[K*(1400)π + Kf] (×).
b) Difference between the total mass spectrum and the combined 1^+S and 2^-S intensity. This shows that apart from 1^+S near 1300 (2^-S near 1700 MeV) other partial waves must be present to build up the Q(L) enhancement.

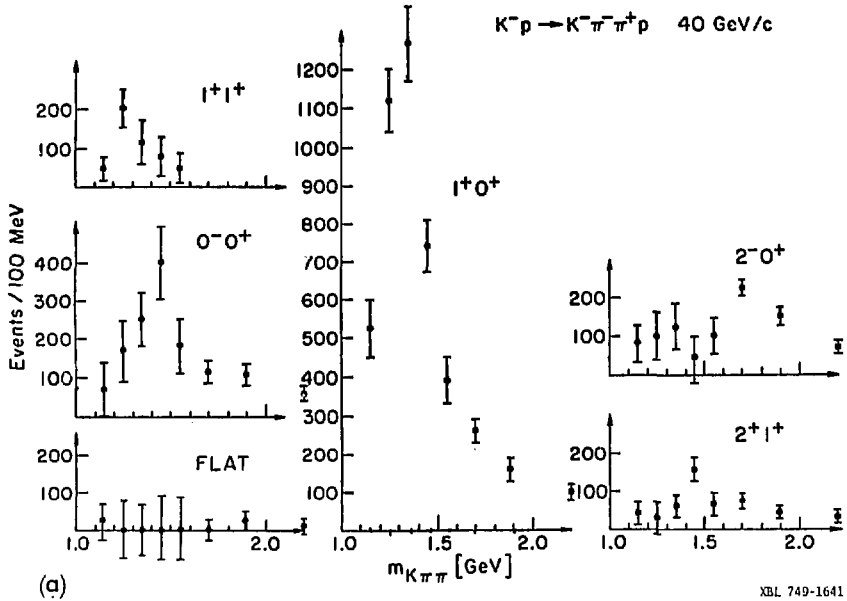

FIG. 26. a) Intensities for various Kππ partial waves as a function of $M_{K\pi\pi}$ from the reaction $K^-p \rightarrow K^-\pi^-\pi^+p$ at 40 GeV/c.[64] The trapezoidal shape of the Q bump is produced by several partial waves peaking at different masses.

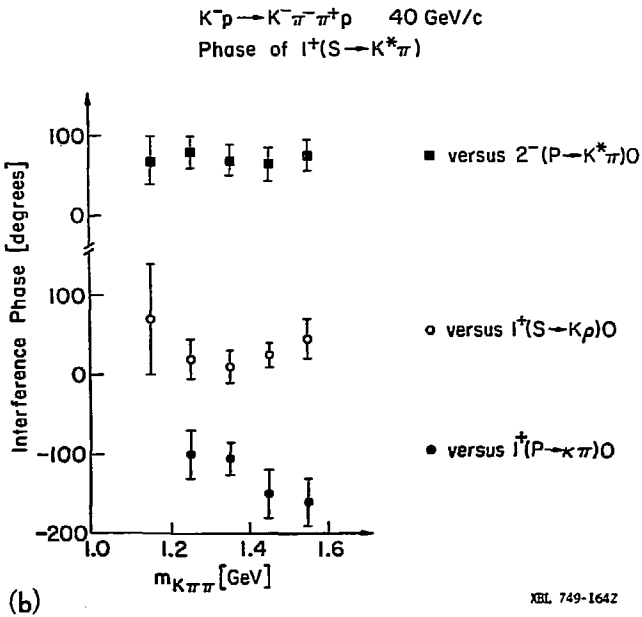

FIG. 26. b) Relative phase of 1^+ $S(K^*\pi)$ against other partial waves as a function of $M_{K\pi\pi}$ showing a similar behavior of the Q as the A_1.

Only the energy dependence behaves differently. In Fig. 25 the mass spectrum of Ref. 62 is given together with the fraction which goes into 1^+ $(K^{*\pm}\pi)$ and 2^- $[K^{*\pm}(1400)\pi]$. These states do not exhaust the Q and the L bump; other states must be present. CIBS-ILL[64] assumed that the analogous states are present as in the 3π system. Their result for break up of the cross section into various partial waves is shown in Fig. 26a. 1^+S $(K^{*\pm}\pi)$ dominates, but there are other smaller partial waves peaking at different places. The complicated shape of the Q bump is then due to a sum of many small partial waves added to the dominating 1^+ S-wave. As in the A_1 case there is not indication for a phase variation of 1^+ over the Q bump region (see Fig. 26b). Also there is no need for two resonances Q_L and Q_H which have been proposed[65] to explain the non-B.W. shape of the Q. The analysis of Ref. 66 more or less confirms these conclusions. Due to the lack of statistics, the final states in many waves are assumed to be phase coherent. Releasing this constraint for the $1^+S(K\rho)$ and $1^+S(K^{*\pm}\pi)$ waves phase coherence seems to be badly violated.[66] This can be finally answered only by experiments which identify π and K.

IV. FORMATION EXPERIMENTS

This field is characterized by many new data, but no reliable analysis has been performed. At the last conference[67] all the narrow S, T, U states claimed by the CBS group[68] have been buried in the background. The first (S) has risen as the new total cross sections from the BNL[69] on $\bar{p}p$ and $\bar{p}d$ show. A narrow bump with probably I = 1 has been observed at M = 1932 ± 2 MeV and $\Gamma = 19 \pm \frac{4}{3}$ MeV. In the following we want to discuss new experiments in the T and U region showing that these states must be much broader. The reactions investigated are:

$$\bar{p}p \to \bar{p}p,\ nn \qquad (4.1a,b)$$

$$\bar{p}p \to \pi^+\pi^-,\ \pi^0\pi^0 \qquad (4.2a,b)$$

$$\bar{p}p \to K^+K^-,\ K_LK_S \qquad (4.3a,b)\ .$$

In reaction (4.3b) at a mass ~ 1970 MeV a structure in the cross section has been reported,[70] which has not been seen by Ref. 71. New data of Ref. 72 favor the result of Ref. 71, as the authors say.

Another way to measure $N\bar{N} \to \pi\pi$ consists in the Chew-Low extrapolation of the reactions

$$\pi^-p \to (\bar{p}p)n \qquad (4.4)$$

$$\pi^-p \to (\bar{p}n)p \qquad (4.5)$$

with a slow n(p). Reaction (4.4) is the only pure π exchange reaction I know of. To see this we can compare the expansion coefficients[73] a_n of the $\cos\theta_{\bar{p}p}$ distribution in terms of Legendre polynomials at small t_{pn} with the corresponding on-shell moments[74] derived from reaction (4.2a). As Fig. 27 shows, both are in reasonable agreement. The coefficients show a typical resonance-dominated energy behavior. Reaction (4.5) has been measured in an experiment with the Ω-spectrometer at 12 GeV/c.[75] The $\cos\theta_{\bar{p}n}$ distribution changes rapidly with $M_{\bar{p}n}$ (Fig. 28a). $\bar{p}n$ is a pure I = 1 state. If only π-exchange contributes, the forward-backward asymmetry should vanish, which is nicely satisfied experimentally (Fig. 28b). For both reactions (4.2a) and $\pi^+\pi^- \to p\bar{p}$ as derived from (4.4), partial wave analyses have been tried.[73,74] No firm conclusion about spin-parity assignment could be drawn except (i) several resonating states together with a complicated background are needed, (ii) if there are any resonances, the daughter level is populated. Certainly polarization experiments can turn $\bar{p}p \to \pi\pi$ into a rich field for resonance hunters. Also the data of the Brown-Bari-MIT collaboration on $\bar{p}p \to \pi^0\pi^0, \eta\pi^0$ in this energy range (results at one energy have been submitted to this conference[76]) are very useful for separating the two isospins. New data on the enhancements ~2.2 GeV (so called T-region) and ~2.4 GeV (U-region) have been reported at this conference [cross section[77] for reaction (4.16) and $\frac{d\sigma}{dt}\ \theta = 180°$ for both reactions (4.1)[78,79]]. The T and U effects are seen as bumps in $\sigma(\bar{p}p \to \bar{n}n)$ (Fig. 29). Figures 30a,b show the backward cross section for $\bar{p}p \to \bar{p}p$[78] and $\bar{p}p \to \bar{n}n$[79] as a function of P_{lab}, indicating a fair amount of resonance production in that region. The T and U enhancements have been observed earlier in several other experiments: $\sigma_t(\bar{p}p)$[80,81] and $\bar{p}p \to \rho^0\rho^0\pi^0$.[82] Table V lists the values for mass, width, and cross section for both enhancements. Since in none of the cases has spin parity been measured, different reactions can very well show different objects.

V. MISCELLANEOUS RESULTS

Various other topics will be covered by the mini-rapporteurs. I will mention only a few results: The spin parity of the $\eta'(960)$ can be still 0^- or 2^-. The Dalitz plot favors 0^-, whereas η' in the $K^-p \to \eta'\Lambda$ data of BNL-Michigan[83] shows anisotropic decay angular distributions in the very forward direction. New data of C. Baltay et al. do not support these anisotropies;[84] for a detailed discussion see Ref. 85. The most puzzling fact is the large ratio R of the electromagnetic decay $\eta' \to \pi^+\pi^-\gamma$ and the strong decay $\eta' \to \pi^+\pi^-\eta$.

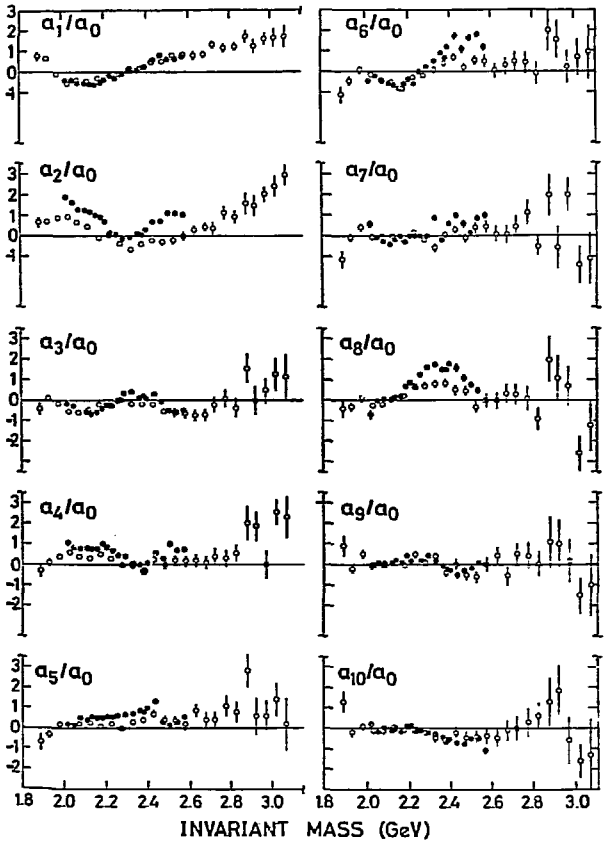

XBL 749-1643

FIG. 27. Legendre coefficients for the differential cross section of $\bar{p}p \to \pi^-\pi^+$ as a function of the invariant mass (● from Ref. 74). The open points are results from the reaction $\pi^- p \to p\bar{p}n$, assuming π exchange.

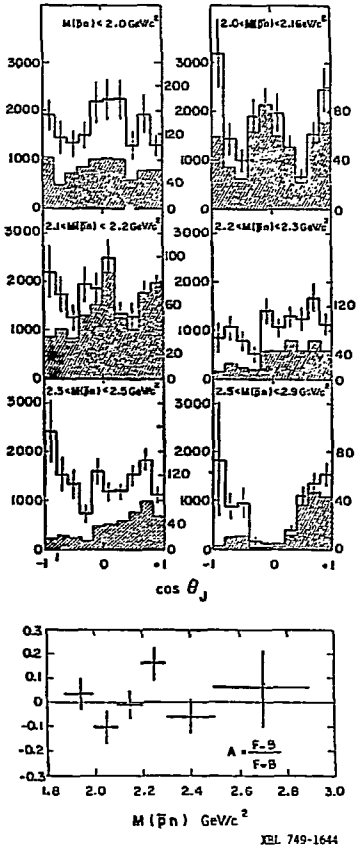

FIG. 28. Cos $\theta^{*}_{\bar{p}n}$ distribution (THS) for the reaction $\pi^- p \to \bar{p}n\, p$ at 12 GeV/c[75] for various $\bar{p}n$ masses. If only π exchange contributes, the forward-backward asymmetry has to vanish, which is shown in the bottom histogram as a function of $M_{\bar{p}n}$.

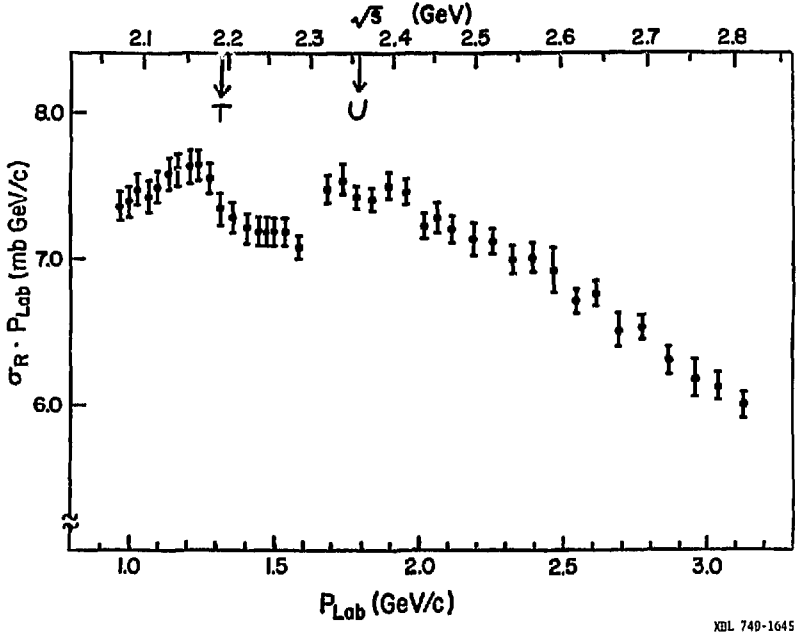

FIG. 29. $\sigma(\bar{p}p \to \bar{n}n) \cdot P_{lab}$ as a function of the laboratory momentum.(77)

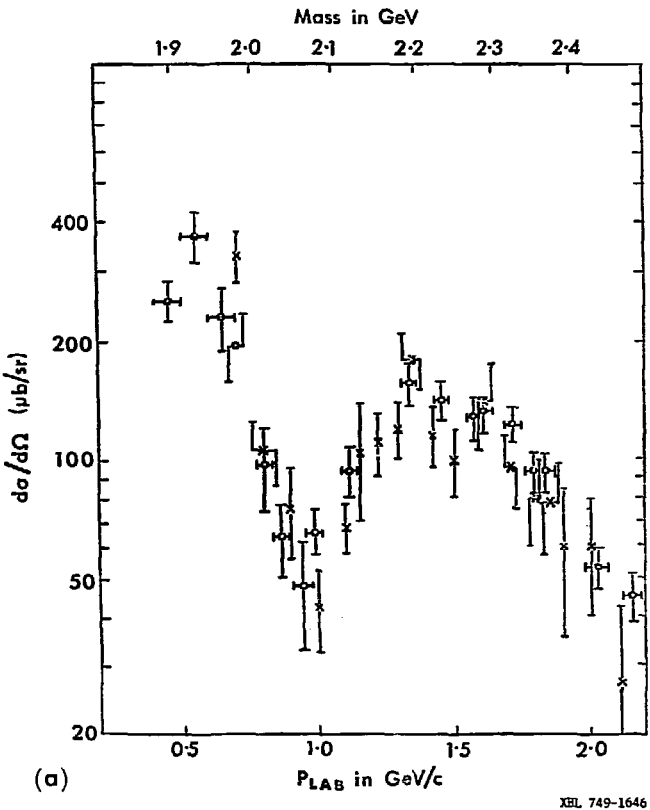

FIG. 30. a) Backward cross section $(d\sigma/d\Omega)_{180°}$ for $\bar{p}p \to \bar{n}n$ as a function of the laboratory momentum [×, Ref. 79; ♦, Ref. 93; ϕ, Ref. 94].

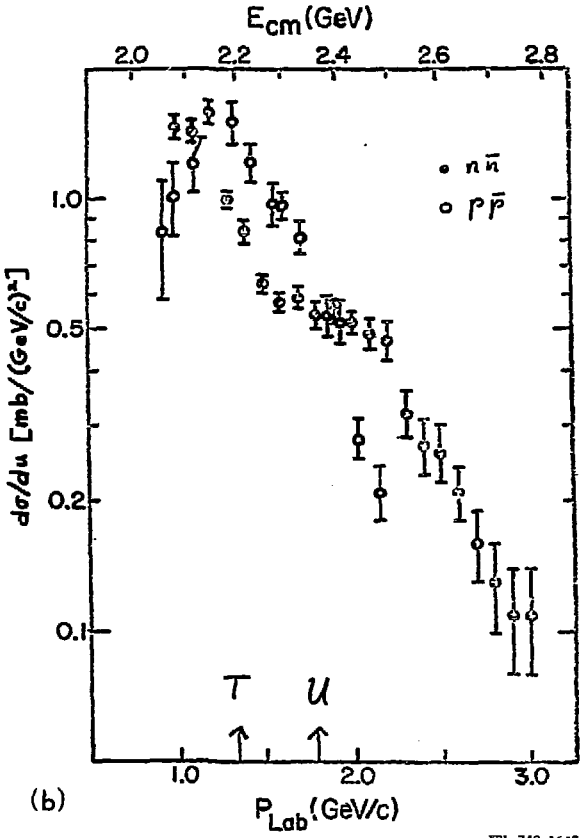

FIG. 30. b) Backward cross section $(d\sigma/du)_{u=0}$ as a function of the laboratory momentum for $\bar{p}p \to \bar{n}n$ (● from Ref. 78) and $\bar{p}p \to \bar{p}p$ (○ from Ref. 94).

TABLE VI. T, U parameter

	RAS[81]	σ_T[80]	$\rho^0\rho^0\pi^0$[85]	$\bar{p}p$-$n\bar{n}$[77]
M_T	2193± 2	2187± 3	~2200	~2150
M_T	98 ± 8	56 ± 8	~60	~50
σ_T(mb)	2.32 ± 0.13	1.85 ± 0.25	1.5-2.0	~0.2
M_U	2360± 2	2363± 2	—	~2360
Γ_U	168 ± 8	171 ± 10	—	~150
σ_U(mb)	2.06 ± 0.20	2.52 ± 0.18	—	?

A recent evaluation based on the world data[85] yields

$$R = 0.87 \pm 0.06 .$$

If η' is indeed 2^-, then the angular momentum barrier would suppress the strong decay.

There are new results on two radiative decays using the Primakoff effect.[86] Browman et al.[87] measured the $\eta \to 2\gamma$ decay rate

$$\Gamma(\eta \to 2\gamma) = 0.324 \pm 0.046 \text{ (keV)},$$

which is 3.5 standard deviations away from the previous value[88] $\Gamma = 1.0 \pm 0.2$ keV. As the authors of Ref. 86 point out, their data are in rough agreement with the raw data of Ref. 87, and they concluded that the background has been underestimated in the old experiment. From coherent production of ρ^- on nuclear targets, B. Gobbi et al.[89] found a value for the radiative decay $\rho^- \to \gamma\pi^-$

$$\Gamma(\rho^- \to \pi^-\gamma) = 35 \pm 10 \text{ keV},$$

which is in poor agreement with the SU_3 prediction of ~100 keV.

Exotic mesons have been searched for and no evidence has been found for their existence. This subject has been reviewed recently by Cohen.[90]

VI. CONCLUDING REMARKS

One of the striking features of meson spectroscopy is the persistent absence of states with spin-parity 0^+, 1^+ ($E, \epsilon, A_1, Q \cdots$) which are needed in the quark model to fill up the $L = 1$ $q\bar{q}$ multiplet. Those states all have in common that they are S-waves in their main decay mode ($\epsilon \to \pi\pi$, $\kappa \to K\pi \cdots$). If we interpret the quark model as providing strong attractive forces in non-exotic channels, the following qualitative argument can give an understanding of why ϵ or κ should not be seen as resonances. If the potential between the two π's has a simple shape with finite range (dashed line in Fig. 31), one can have for the S-wave either a bound state for strong coupling or a strong phase shift for smaller couplings, but not a resonance, which requires a repulsive wall in order to trap an unstable state. Such a wall is provided by the angular momentum barrier for P and higher waves (dotted line in Fig. 31), which gives the shape as indicated by the solid line when added to the potential. Such an effective potential can easily give a resonance. This explains how one can reconcile the observed strong S-interaction in both $\pi\pi$ and $K\pi$ with the quark model.

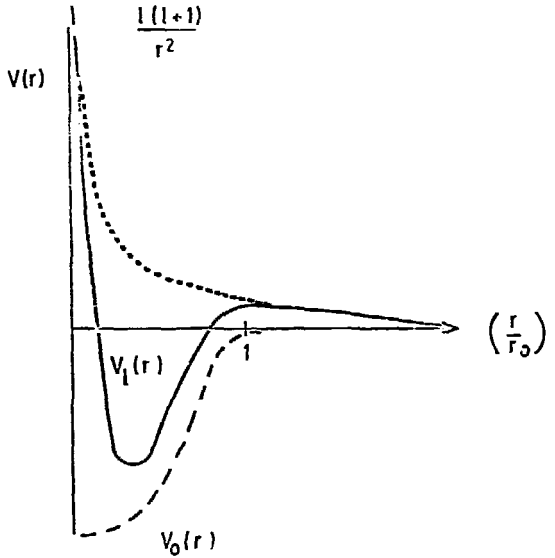

FIG. 31. Potential of range r_0 (dashed line). The dotted line gives the centrifugal barrier and the solid line the sum of both.

ACKNOWLEDGMENTS

I am especially indebted to the members of group A(LBL) for providing me the data of their $\pi^{\pm}p$ (7-GeV/c) and $K^{\pm}p$ (12-GeV/c) experiments on which Figs. 7, 16, and 27 are based. I would like to thank Professor Ascoli and the members of the CERN-Munich group for discussions and the help in preparing figures. I am grateful to Dr. Morrison for discussions. In particular, I want to acknowledge the help I received from Professor Colley and the scientific secretaries Dr. S. M. Jones and B. Kelley in preparing this report.

FOOTNOTES AND REFERENCES

Batavia[72] abbreviates: Proceedings of the XVI International Conference on High Energy Physics, NAL 1972, edited by T. D. Jackson and A. Roberts. EMS 74 abbreviates: Experimental Meson Spectroscopy 1974, Boston. Contributions to this conference are indicated "paper A" (A is the number, NN stands for post-deadline contributions).

1. G. C. Fox et al., Nucl. Phys. B56, 386 (1973).
2. G. L. Kane, paper 184.
3. G. F. Chew et al., Phys. Rev. 113, 1640 (1959).
4. S. Protopopescu et al., Phys. Rev. D 7, 1279 (1973).
5. G. Grayer et al., Nucl. Phys. 1974.
6. W. Männer, paper NN and invited talk at EMS 74.
7. C. F. Cho et al., Phys. Lett. 30B, 119 (1969).
8. P. K. Williams, Phys. Rev. D 1, 1312 (1970); G. C. Fox, Proc. Cal. Techn. Conference on Phenomenology in Particle Physics, Pasadena, 1971.
9. P. Estabrooks et al., Phys. Lett. 41B, 350 (1972).
10. W. Ochs, Nuovo Cimento 12A, 724 (1972).
11. W. Ochs, Thesis, Munich, 1973; B. Hyams et al., Nucl. Phys. B64, 134 (1973).
12. P. Estabrooks et al., paper 578. This replaces the earlier publication of Ref. 12a.

12a. P. Estabrooks et al., Proceedings of the Tallahassee Conference on $\pi\pi$ Scattering, AIP No. 13 (1973), p.37.

13. P. Estabrook et al., paper 579.
14. J. L. Basdevant et al., preprint, Paris, 1973.
15. W. Hoogland et al., Nucl. Phys. B69, 266 (1974).
16. S. Weinberg, Phys. Rev. Lett. 17, 616 (1966).
17. Private communication of Dr. Yndurain. See also K. Kleinknecht's talk at this conference.
18. H. Nielsen et al., Nucl. Phys. B72, 321 (1974).
19. J. A. Jones et al., paper 430.
20. Y. Lemoigne et al., paper NN.
21. G. Grayer et al., Nucl. Phys. B50, 29 (1972).
22. F. Wagner, paper 266.
23. L. Stodolsky, Phys. Rev. 134, B1099 (1964).
24. A. Bialas et al., Nucl. Phys. B6, 465, 478 (1968).

25. F. Wagner, to be published.
26. See compilation in Ref. 15.
27. Villet et al., Saclay 1973 (points at higher $M_{\pi\pi}$ are left out); M. Losty et al., Nucl. Phys. B69, 185 (1974); E. Colton et al., Phys. Rev. D 3, 2028 (1971).
28. J. P. Prukop et al., paper 688.
29. E. Barrelet, Nuovo Cimento 8A, 331 (1972).
30. C. D. Frogatt et al., paper 384.
31. E. Pietarinen, Nuovo Cimento 12A, 522 (1972).
32. M. Roos, Helsinki preprint 63-1973.
33. H. Bingham et al., Phys. Lett 41B, 635 (1972).
34. G. Barberino et al., Lett. Nuovo Cimento D 6, 2374 (1972); C. Bacci et al., Phys. Lett. 38, 551 (1972).
35. W. Beusch et al., paper NN.
36. M. Aguilar-Benitez et al., papers 444 and 923.
37. A. J. Pawlicki et al., paper 98.
38. J. Dowell et al., paper 233.
38a. M. J. Matison et al., Phys. Rev. D 9, 1872 (1974).
39. G. W. Brandenburg et al., paper 235.
40. PDG, Phys. Lett. 50B, 1 (1974).
41. D. D. Carmony et al., Phys. Rev. Lett. 27, 1160 (1971); A. Firestone et al., Phys. Lett. 36B, 513 (1971); M. Aguilar-Benitez Phys. Rev. Lett. 30, 672 (1973).
42. ABCLV - Collaboration paper 421.
42a. D. Cords et al., Nucl. Phys. B54, 109 (1973).
43. For an attempt see P. V. Chliapnikov et al., paper NN.
44. G. Ascoli et al., Phys. Rev. Lett. 25, 962 (1970); Phys. Rev. Lett. 26, 929 (1971); Phys. Rev. D 7, 669 (1973).
45. See, e.g., J. D. Hansen et al., CERN/D. Ph. II/Phys. 73-34.
46. M. Tabak et al., paper 889.
47. CIBS, Nucl. Phys. B63, 153 (1973).
48. G. Thomson et al., Nucl. Phys. B69, 381 (1974).
49. AB^2CLV collaboration, paper 423.
50. E. Kruse et al., paper 671.
51. M. J. Emms et al., paper 400.
52. S. J. Lindenbaum et al., paper 134.
53. C. Michael, Batavia 1972 rapporteur's talk.

54. M. Losty et al., private communication by V. Chaloupka, $\sigma_{nat}(A_2) = 8.0 \pm 1$ μb at 3.9 GeV/c; CERN-Munich group, private communication by H. Dietl: $\sigma_{nat}(A_2) = 5.7 \pm 0.6$ μb at 9.8 GeV/c and 3.2 ± 0.2 μb at 18.9 GeV/c.
55. F. A. Bianca et al., paper 206.
56. D. Chew et al., in preparation.
57. P. Hoyer et al., Nucl. Phys. B56, 173 (1973).
58. G. Ascoli et al., Phys. Rev. D 9, 1963 (1974).
59. G. Ascoli et al., paper 666 and COO-1195-285 (1974).
60. M. Bowler, paper NN.
61. S. Dado et al., paper 104.
62. ABCLV collaboration, paper 424, Phys. Lett. 49B, 388 (1974).
63. A^2BCL^2V collaboration, paper 422.
64. CIBA-ILL collaboration, paper 666.
65. A. Firestone et al., EMS 70.
66. S. N. Tovey et al., paper 47.
67. W. Kienzle et al., EMS 72.
68. Focacci, et al., Pbys. Rev. Lett. 17, 890 (1966).
69. A. S. Carroll et al., Phys. Rev. Lett. 32, 247 (1974).
70. Benvenuti et al., Phys. Rev. Lett. 27, 283 (1972).
71. Carson et al., Batavia 72 paper 498.
72. M. Aguilar-Benitez et al., paper 445.
73. B. Hyams et al., Nucl. Phys. B73, 202 (1974).
74. E. Eisenhandler et al., Phys. Lett. 47B, 531, 536 (1973).
75. B. Ghidini et al., paper NN.
76. R. E. Lanou et al., paper NN.
77. D. Cutts et al., paper 731.
78. J. Storer et al., paper 732.
79. E. Eisenhandler et al., paper 712.
80. Abrams et al., Phys. Rev. Lett. 18, 1209 (1967).
81. J. Alspector et al., Phys. Rev. Lett. 30, 511 (1973).
82. For a critical review see G. Kalbfleisch, EMS 74.
83. J. S. Danburg et al., Phys. Rev. D 8, 3744 (1973).
84. C. Baltay et al., paper 909.
85. G. Kalbfleisch, EMS 74.
86. W. Primakoff, Phys. Rev. 81, 899 (1959).
87. A. Browman et al., Phys. Rev. Lett. (1974).
88. C. Bemporard et al., Phys. Lett. 35B, 380 (1967).

89. B. Gobbi et al., paper 772.
90. D. Cohen, EMS 74.
91. Binnie et al., Phys. Rev. Lett. 31, 1534 (1973). Threshold MM spectrometer.
92. G. Grayer et al., Tallahassee Conference, 1973. Fit to 17 GeV/c CERN-Munich $\pi\pi$ elastic and $\pi\pi \to K\bar{K}$ data.
93. D. Cline et al., Phys. Rev. Lett. 21, 1268 (1968).
94. J. K. Yoh et al., Phys. Rev. Lett. 23, 506 (1969).